

Understanding Inks for Porous-Electrode Formation

Kelsey B. Hatzell,¹ Marm B. Dixit,¹ Sarah A. Berlinger,² Adam Z. Weber²

¹Department of Mechanical Engineering, Vanderbilt University, Nashville, TN, 37235, USA

²Energy Technologies Area, Lawrence Berkeley National Laboratory, Berkeley, CA, 94720, USA

Scalable manufacturing of high-aspect-ratio multi-material electrodes are important for advanced energy storage and conversion systems. Such technologies often rely on solution-based processing methods where the active material is dispersed in a colloidal ink. To date, ink formulation has primarily focused on macro-scale process-specific optimization (i.e. viscosity and surface/interfacial tension), and been optimized mainly empirically. Thus, there is a further need to understand nano- and mesoscale interactions and how they can be engineered for controlled macroscale properties and structures related to performance, durability, and material utilization in electrochemical systems.

Porous electrodes are ubiquitous in various electrochemical technologies, yet their genesis still resides mainly in the empirical domain. Similarly, printable and nano-materials processing has seen rapid improvements in the last decade,¹⁻³ enabling precise control over 1D, 2D, and 3D structural properties. This has allowed for the development of printed microcapacitors for integration into flexible and wearable electronics^{4,5}. Broadly however, the feedstock material has yet to be optimized fully. Technologically, formation of electrodes encompasses a variety of processing techniques including ink-jet printing, transfer printing, spray-coating, stamping, and screen printing from an ink. An ink broadly encompasses a material(s) to be printed or coated and a carrier fluid that is removed by evaporation during the solidification or curing process (**Fig. 1**).⁶ Electrodes in batteries and catalyst layers in fuel cells and electrolyzers are manufactured via solution-processed approaches and both the ink formulation (**Fig. 1b**) and fabrication method (**Fig. 1c**) play a role in determining the microstructure, underlying material arrangement, capacity, and activity of an electrode system.^{7, 8} However, detailed control of microstructure, active and inactive material distribution, and morphology, which are needed for better utilization and next-generation architectures,⁹⁻¹¹ remains unlinked for the most part to the ink descriptors. Understanding and tailoring the ink properties, so called ink engineering, allows for precise control over the eventual multicomponent composite structures. Herein, we highlight recent and specific works that seek to discern the governing interactions between the polymer, active material, and solvents in electrode inks and ultimately how they can be engineered for processing^{6, 12, 13}.

Inks for battery electrodes and catalyst layers are similar and are comprised of an active material, a polymer, and a carrier fluid (solvent). In batteries, the active material can be a range of inorganic crystalline materials^{14, 15}, amorphous organosulfur compounds¹⁶, or metalloids (silicon)¹⁷, while in fuel cells and electrolyzers the active material is an amorphous or graphitized carbon material decorated with a nano-catalyst material.¹⁸ Both electrode systems have a polymer that serves as the binder that holds individual particles together and to the substrate. The binder can also be functionalized to provide ion or electron conductance as well as providing the mechanical integrity (durability) of the electrode during electrochemical operation.^{19, 20} The polymer loading in a fuel-cell catalyst layer can be on the order of 40 to 60 v% (30 to 50 wt%)^{21, 22} while the polymer loading is typically minimized in battery applications (5 to 10wt%) (**Fig. 2b**). Thus, the catalyst-layer microstructure is polymer-driven and the battery-electrode microstructure is less affected by polymer content. In both applications however, the biphasic and ternary nature of these dispersions induce complex interactions that affect the deposition or coating process,^{23, 24} and how inks are transformed during relevant coating processes (**Fig. 1b-c**)²⁵. Furthermore, ink formulations are typically empirically optimized with parametric studies that are often unique to these coating processes (**Fig. 2a**)²⁶. In batteries, it is important to have good packing density and low additive content for favorable volumetric energy densities^{27, 28}, while in fuel-cell electrodes, the secondary pores²⁹ are necessary to facilitate gas transport (**Fig. 1d**). Controlling electrode properties during formation requires both control over interactions between the materials in the ink phase (colloidal form) and during shear processing (printing)¹³.

Within an ink, interactions include particle|polymer, solvent|particle and polymer|solvent ones. Poly(vinylidene) fluoride (PVdF), carboxymethyl cellulose (CMC), and polyvinyl alcohol (PVA) are common polymers used as binders in battery applications^{30, 31} and a proton conducting polymer (e.g., perfluorosulfonic acid (PFSA))³² or hydroxide-conducting ionomer is used in catalyst layers. A good polymer for electrochemical applications is characterized by a high adhesion strength in order to avoid delamination and an ability to swell and uptake electrolyte for effective ionic transport¹⁹. Electrode durability and performance in battery systems is dependent on achieving a homogeneous distribution of the polymer throughout the electrode volume.^{33, 34} While in catalyst layers, better performance is obtained with precise, percolated ionomer distribution.^{35, 36} The polymer can inhibit solid-electrolyte-interphase growth at the covered active material surfaces.³⁷ Also, active materials with surface functionalities that induce strong hydrogen-bond interactions have been shown to increase binder distribution throughout the bulk of electrode systems.^{33, 38, 39} This was observed when comparing PVdF and a hydroxyl-modified PVdF binder in graphite electrodes systems. The hydroxyl-modified PVdF system led to more homogenous structure due to stronger interactions with the graphite in the ink phase.³³

Polymer|solvent interactions can affect the formation of effective three-phase boundary interfaces in catalyst layers during coating processes. There have been significant efforts to optimize and innovate the polymer in terms of properties (conductivity), structure, molecular weight, durability, and cost.¹⁹ In addition, recent research efforts include discerning the effect of the solvent on the structure and functional properties in electrode systems³¹. Specifically, the mobility of the polymer in a solvent,⁴⁰ the degree of chain entanglement in the solvent,⁴¹ and the

colloidal morphological form of the polymer⁴² have all been identified as important properties for creating effective catalyst layers. The dielectric constant (ϵ) of a solvent can result in different polymer conformations which can change the structural morphology of the polymer in both solution and cast phases. PFSA forms a solution ($\epsilon > 10$), a colloid ($3 < \epsilon < 10$), or a precipitate ($\epsilon < 3$)^{35,43} based on the designed solvent.

However, PFSA does not exhibit true solution behavior. Rather, with the aid of small angle neutron scattering (SANS), it was demonstrated that high ϵ solvents can produce different PFSA conformations depending on solvent choice: random coils in NMP; large, swollen clusters in water propanol mixtures; and cylindrical particles in glycerol.⁴⁴ Furthermore, Kim et al. correlated the solvent in Nafion dispersions to cast film mechanical properties⁴¹. They found three different gelation modes (thermally reversible gelation in most aprotic solvents, thermally irreversible gelation that formed a precipitate in water/monohydric alcohol mixtures, and thermally irreversible gelation that forms a film in pure alcohols) upon solvent evaporation, and found good agreement of critical gelation concentration (CGC) with mechanical toughness for the different gelation modes. CGC is related to the degree of chain entanglements, which they identified as the main indicator of mechanical toughness, rather than percent crystalline area.^{41, 44}

45

Furthermore, PFSA as a colloid can preferential interact with Pt active sites rather than carbon surfaces and thus results in localized distribution of the polymer. These observations have been supported by DFT measurements that estimate a lower adsorption energy for sulfonic acid functional groups on platinum than carbon⁴⁶. Shin et al. further showed that PFSA in a colloid form led to higher porosities in the electrode structure which demonstrated reduced mass-

transport and ohmic resistances.³⁶ Uchida et al. similarly found that this preparation method increased the surface area between the platinum and the ionomer, and had greater continuity of the ionomer network yielding higher catalyst utilization.³⁵ However, other groups have analyzed solution and colloidal Nafion and found solution-based forms to exhibit the highest cell performance due to even ionomer distribution.^{47, 48} Discrepancies between the groups could possibly be explained by casting process differences; the groups that found colloidal Nafion to be preferable cast their catalyst layers on gas diffusion media, while the groups that saw the opposite cast on the membrane or a decal. Regardless, this underscores the necessity of understanding individual interactions between components in an ink and global ink properties (rheological behavior) are important for manufacturing electrodes with: (1) high adhesion strength, (2) low tortuosity, and (3) processability.

Aside from polymer|solvent interactions, polymer|particle and solvent|particle interactions govern the aggregation size, processability, and materials arrangement in an electrode system. For example, molecular-dynamics studies have shown that ionized graphite sheets are more likely to adsorb ionomers (PFSA) than bare graphite sheets, and the ionomer coverage is solvent- and polymer equivalent weight-dependent.⁴⁹ Within the field of organic field-effect transistors, polymer side-chain engineering has been explored as a route for altering the physical properties of organic devices and there is the same potential in electrochemical systems to tailor polymers for controlled interactions. The potential to control these interactions may provide a means for spatial control over polymer and solid materials within electrodes via polymer-mediated self-assembly³.

Furthermore, one must consider not only the zero-time composition of the ink, but also its stability to improve and allow for reproducible coatings.^{13, 50} Recently, it was shown that the high polymer loading in carbon-based inks can increase the shelf-life or stability, which suggests that the polymer (perfluorosulfonic acid in fuel cells) acts as a stabilizing agent.⁵¹ From a colloidal perspective, stability describes the ability to disperse a nano-material within a desired solvent which can be accomplished by controlling the energy exchanged between colliding particles in an ink or colloid systems^{52, 53}. In electrochemical systems, the ink needs to be engineered for colloidal stability as well as material stability. Oxidation or dealloying of the solid active material in an ink phase prior to coating or manufacturing processes can decrease the energy storage capacity or power density of an electrode⁵⁴. Koh et al., demonstrated that liquid aqueous catalyst inks displayed optimal electrocatalytic properties after being aged for 24 to 48 hours⁵⁴ and showed performance decreases after 48 hours. The increase in performance was attributed to increased wetting of the active sites, and decreases in performance over time was attributed to aggregation and phase separation of constituent components. While there are extensive studies which elucidate aging in dry materials, there are far less that probe ink aging. For advanced materials processing an understanding about the underlying ink interactions is important.

Inks as colloidal materials are considered far-from-equilibrium material systems and require a suite of characterization techniques to probe effectively their structure, function, and properties at multiple lengthscales. While individual ink components are extensively characterized, less characterization is completed on the ink as a whole. This is in part because inks cannot be probed

with traditional imaging or stationary interrogation techniques due to their opacity and multiphasic nature. Despite these limitations, numerous techniques have emerged as effective strategies for characterizing key ink properties (see **Fig. 3**): viscosity, surface tension, ink structure, material morphology, and solid material aggregation size. Broadly, material characterization techniques can be divided into direct and indirect techniques. Direct techniques refer to methods that produce data that is completely observable, whereas indirect techniques typically require empirical models to evaluate material properties. Recently, Takahashi et al. used cryogenic scanning electron microscopy (cryo-SEM) to observe both ink aggregation⁵⁵ and ionomer distribution within the ink⁵⁶. They confirmed that cryo-SEM measurements matched the particle size distribution obtained by laser diffraction, and that water/propanol based inks at concentrations studied exhibited bimodal aggregate sizes. Furthermore, they observed the ionomer in inks with and without platinum and noted an increased ionomer density around particles containing platinum compared with those of pure carbon. Despite these findings, cryogenic-based visualization methods pose two primary challenges: (1) solvent loss (compositional uncertainty) and (2) the introduction of structural artifacts due the growth of ice crystals that can be somewhat minimized by plunging into liquid ethane or similar solutions. Two other techniques that can enable direct structural observations under non-equilibrium conditions include synchrotron x-ray tomography⁵⁷ and confocal laser scanning microscopy,⁵⁸ but they are limited to micrometer-level lengthscales and are thus primarily useful for understanding segregation, aging, and aggregation phenomena. For smaller feature probes, one can use small angle x-ray scattering and neutron-scattering methods.^{47, 59-61} Functional characteristics like the particle size, morphology, and size distribution can be obtained from

fitting the Porod and Guinier regions of the intensity profiles with models. Additionally, advanced neutron scattering techniques that combine standard rheological techniques with neutron scattering (Rheo-SANS) provide unique insight into ink properties.⁶² Most of these techniques still rely on interpretation and average sizes; direct imaging techniques remain a need.

Similar to experimental diagnostics, modeling of the formation process and interactions within the inks is still in its infancy for these processes. DLVO theory has been used to describe ink stability and interactions^{51, 63}, yet it does not necessarily account for rheological effects. Similarly, coarse-grained models of catalyst-layer inks have revealed that as the dielectric constant of the solvent increases, the agglomerate size (solid material) decreases within an ink due to decreases in the ionomer cluster size,⁶⁴ although experimental evidence of this fact is less conclusive (**Fig. 2c**).^{51, 56, 60, 65-71} This highlights the need for more detailed experiments to inform the model physics and parameters. For the complete process of ink to casting to electrode microstructure, there is a need for a multiscale, multiphysics description. Of note is the recent modeling work of Wheeler and coworkers⁷² that attempts this for battery electrodes and is promising; more efforts like these are required to help uncover the key processes and interactions and strive towards predictive models.

As noted, it is not just the inherent dispersion interactions within the ink that control the electrode formation, but also the casting method. There are several means for processing high areal electrode systems including, but not limited to, painting, doctor blade, ink-jet, slot-die, and spray coating. Each of these processes can be transformed into or already exist at roll-to-roll

scale. Under these different methods, the inks undergo many different shear regimes (see **Fig. 4c**), since depending on the polymer and solid content loading, electrode inks can be considered viscous or viscoelastic materials. Generally, the processing technique introduces two limits: ink viscosity and achievable process speed (**Fig. 4a**). Moreover, each of these processes subject the 'ink' to different shear environments ranging from low shear rate processes such as brush or rolling to high shear environments such as spray coating. The primary deformation mode for spray processing methods is extensional (not shear), whereas traditional coating mechanisms based on roll or blade coating are subject to standard shear dynamics (**Fig. 4b**). For Newtonian inks or liquids, the extensional forces are only ~3X that of shear viscosities, but for complex fluids (non-Newtonian) the extensional viscosity can be 10^4 times greater than the shear rate⁷³⁻⁷⁵ and can result in polymer alignment and different material properties (**Fig. 4c**). Furthermore, viscosity studies have previously been used to model fundamental binary interactions⁷⁶, but not much work has been done applying this to fuel cell or battery inks. These rheological impacts have only recently begun to be examined in a systematic fashion.

In summary, there is a growing need for fabricating porous electrodes with unprecedented control of layer composition⁷⁷. Key to this is knowledge of the underlying physics and phenomena going from multicomponent dispersions and inks to casting/processing to 3-D structure. While there has been some recent work as highlighted herein, a great deal remains to be accomplished in order to inform predictive and not empirical optimizations. Such investigations have occurred in other fields such as semiconductors and coatings and dispersions in general, but this has not been translated to thin-film properties and functional layers as occur

in electrochemical devices. Overall, ink engineering is an exciting opportunity to achieve next-generation composite materials, but requires systematic studies to elucidate design rules and metrics and identify controlling parameters.

Acknowledgements

M.B.D and K.B.H were supported by the National Science Foundation under Grant No. 1727863. K.B.H acknowledges support from the Ralph E. Powe Junior Faculty Enhancement Award from ORAU. S.A.B. and A.Z.W. were supported by the Fuel Cell Performance and Durability Consortium (FC-PAD), of the Fuel Cell Technologies Office (FCTO), Office of Energy Efficiency and Renewable Energy (EERE), of the U.S. Department of Energy under contract number DE-AC02-05CH11231.

References

1. M. Ha, Y. Xia, A. A. Green, W. Zhang, M. J. Renn, C. H. Kim, M. C. Hersam and C. D. Frisbie, *ACS nano*, 2010, **4**, 4388-4395.
2. J. Rogers and H. Katz, *Journal of Materials Chemistry*, 1999, **9**, 1895-1904.
3. J. Mei and Z. Bao, *Chemistry of Materials*, 2013, **26**, 604-615.
4. Y. Yue, Z. Yang, N. Liu, W. Liu, H. Zhang, Y. Ma, C. Yang, J. Su, L. Li, F. Long, Z. Zou and Y. Gao, *ACS Nano*, 2016, **10**, 11249-11257.
5. S. Wang, N. Liu, J. Tao, C. Yang, W. Liu, Y. Shi, Y. Wang, J. Su, L. Li and Y. Gao, *Journal of Materials Chemistry A*, 2015, **3**, 2407-2413.
6. J. Li, B. L. Armstrong, C. Daniel, J. Kiggans and D. L. Wood, *Journal of colloid and interface science*, 2013, **405**, 118-124.
7. W. K. Epting, J. Gelb and S. Litster, *Advanced Functional Materials*, 2012, **22**, 555-560.
8. V. P. Nemani, S. J. Harris and K. C. Smith, *Journal of The Electrochemical Society*, 2015, **162**, A1415-A1423.
9. A. Z. Weber and A. Kusoglu, *Journal of Materials Chemistry A*, 2014, **2**, 17207-17211.
10. T. A. Greszler, D. Caulk and P. Sinha, *Journal of The Electrochemical Society*, 2012, **159**, F831-F840.
11. A. Phillips, M. Ulsh, J. Porter and G. Bender, *Fuel Cells*, 2017.
12. J. Li, B. L. Armstrong, J. Kiggans, C. Daniel and D. L. Wood III, *Langmuir*, 2012, **28**, 3783-3790.
13. J. Li, C. Daniel and D. Wood, *Journal of Power Sources*, 2011, **196**, 2452-2460.
14. J. B. Goodenough and Y. Kim, *Chemistry of Materials*, 2009, **22**, 587-603.
15. K. Mizushima, P. Jones, P. Wiseman and J. B. Goodenough, *Materials Research Bulletin*, 1980, **15**, 783-789.
16. S. Evers and L. F. Nazar, *Accounts of chemical research*, 2012, **46**, 1135-1143.
17. M.-H. Park, M. G. Kim, J. Joo, K. Kim, J. Kim, S. Ahn, Y. Cui and J. Cho, *Nano letters*, 2009, **9**, 3844-3847.
18. E. Passalacqua, F. Lufrano, G. Squadrito, A. Patti and L. Giorgi, *Electrochimica Acta*, 2001, **46**, 799-805.
19. M. Wu, X. Xiao, N. Vukmirovic, S. Xun, P. K. Das, X. Song, P. Olalde-Velasco, D. Wang, A. Z. Weber and L.-W. Wang, *Journal of the American Chemical Society*, 2013, **135**, 12048-12056.
20. B. C. Steele and A. Heinzl, *Nature*, 2001, **414**, 345-352.
21. X. Zhao, W. Li, Y. Fu and A. Manthiram, *international journal of hydrogen energy*, 2012, **37**, 9845-9852.
22. S. M. Andersen, R. Dhiman and E. Skou, *Journal of Power Sources*, 2015, **274**, 1217-1223.
23. J. A. Lewis, *Journal of the American Ceramic Society*, 2000, **83**, 2341-2359.
24. R. Poling-Skutvik, K. I. S. Mongcopa, A. Faraone, S. Narayanan, J. C. Conrad and R. Krishnamoorti, *Macromolecules*, 2016, **49**, 6568-6577.
25. S. Mauger, K. Neyerlin, J. Stickel, M. Ulsh, K. More and D. Wood, *Material-Process-Performance Relationships for Roll-to-Roll Coated PEM Electrodes*, NREL (National Renewable Energy Laboratory (NREL), Golden, CO (United States)), 2017.

26. D. L. Wood III, J. D. Quass, J. Li, S. Ahmed, D. Ventola and C. Daniel, *Drying Technology*, 2017.
27. A. S. Aricò, P. Bruce, B. Scrosati, J.-M. Tarascon and W. Van Schalkwijk, *Nature materials*, 2005, **4**, 366-377.
28. Y. Sun, N. Liu and Y. Cui, *Nature Energy*, 2016, **1**, 16071.
29. S. Holdcroft, *Chemistry of Materials*, 2013, **26**, 381-393.
30. S. Lux, F. Schappacher, A. Balducci, S. Passerini and M. Winter, *Journal of the Electrochemical Society*, 2010, **157**, A320-A325.
31. M. Osinska-Broniarz, A. Martyła, L. Majchrzycki, M. Nowicki and A. Sierczynska, *European Journal of Chemistry*, 2016, **7**, 182-186.
32. S. Sambandam and V. Ramani, *Physical Chemistry Chemical Physics*, 2010, **12**, 6140-6149.
33. M. Yoo, C. W. Frank, S. Mori and S. Yamaguchi, *Chemistry of materials*, 2004, **16**, 1945-1953.
34. J.-H. Lee, U. Paik, V. A. Hackley and Y.-M. Choi, *Journal of Power Sources*, 2006, **161**, 612-616.
35. M. Uchida, Y. Aoyama, N. Eda and A. Ohta, *Journal of The Electrochemical Society*, 1995, **142**, 463-468.
36. S.-J. Shin, J.-K. Lee, H.-Y. Ha, S.-A. Hong, H.-S. Chun and I.-H. Oh, *Journal of power sources*, 2002, **106**, 146-152.
37. J.-i. Yamaki, H. Takatsuji, T. Kawamura and M. Egashira, *Solid State Ionics*, 2002, **148**, 241-245.
38. M. Yoo, C. W. Frank and S. Mori, *Chemistry of materials*, 2003, **15**, 850-861.
39. M. Yoo, C. W. Frank, S. Mori and S. Yamaguchi, *Polymer*, 2003, **44**, 4197-4204.
40. T.-H. Kim, J.-Y. Yi, C.-Y. Jung, E. Jeong and S.-C. Yi, *International Journal of Hydrogen Energy*, 2017, **42**, 478-485.
41. Y. S. Kim, C. F. Welch, R. P. Hjelm, N. H. Mack, A. Labouriau and E. B. Orler, *Macromolecules*, 2015, **48**, 2161-2172.
42. M. Uchida, Y.-C. Park, K. Kakinuma, H. Yano, D. A. Tryk, T. Kamino, H. Uchida and M. Watanabe, *Physical Chemistry Chemical Physics*, 2013, **15**, 11236-11247.
43. Z. Qi and A. Kaufman, *Journal of Power Sources*, 2003, **113**, 37-43.
44. C. Welch, A. Labouriau, R. Hjelm, B. Orler, C. Johnston and Y. S. Kim, *ACS Macro. Lett.*, 2012, **1**, 1403-1407.
45. J. Y. Kim, S. Lee, T.-Y. Kim, C. Pak and H.-T. Kim, *Carbon*, 2014, **77**, 525-537.
46. A. S. Rad and D. Zareyee, *Vacuum*, 2016, **130**, 113-118.
47. F. Yang, L. Xin, A. Uzunoglu, L. Stanciu, J. Ilavsky, S. Son and J. Xie, *ECS Transactions*, 2016, **75**, 361-371.
48. A. Therdthianwong, P. Ekdharmasuit and S. Therdthianwong, *Energy Fuels*, 2010, **24**, 1191-1196.
49. T. Mashio, A. Ohma and T. Tokumasu, *Electrochimica Acta*, 2016, **202**, 14-23.
50. D. Mohanty, E. Hockaday, J. Li, D. Hensley, C. Daniel and D. Wood, *Journal of Power Sources*, 2016, **312**, 70-79.
51. S. Shukla, S. Bhattacharjee, A. Weber and M. Secanell, *Journal of The Electrochemical Society*, 2017, **164**, F600-F609.

52. D. H. Everett, *Basic principles of colloid science*, Royal society of chemistry, 2007.
53. J. N. Israelachvili, *Intermolecular and surface forces*, Academic press, 2015.
54. S. Koh and P. Strasser, *Journal of The Electrochemical Society*, 2010, **157**, B585-B591.
55. S. Takahashi, T. Mashio, N. Horibe, K. Akizuki and A. Ohma, *ChemElectroChem*, 2015, **2**, 1560-1567.
56. S. Takahashi, J. Shimanuki, T. Mashio, A. Ohma, H. Tohma, A. Ishihara, Y. Ito, Y. Nishino and A. Miyazawa, *Electrochimica Acta*, 2017, **224**, 178-185.
57. K. B. Hatzell, J. Eller, S. L. Morelly, M. H. Tang, N. J. Alvarez and Y. Gogotsi, *Faraday Discussions*, 2017.
58. A. Mohraz, E. R. Weeks and J. A. Lewis, *Physical Review E*, 2008, **77**, 060403.
59. F. Xu, H. Zhang, D. Ho, J. Ilavsky, M. Justics, H. Petrache, L. Stanciu and J. Xie, *ECS Transactions*, 2011, **41**, 637-645.
60. F. Xu, H. Zhang, J. Ilavsky, L. Stanciu, D. Ho, M. J. Justice, H. I. Petrache and J. Xie, *Langmuir*, 2010, **26**, 19199-19208.
61. F. Yang, L. Xin, A. Uzunoglu, Y. Qiu, L. Stanciu, J. Ilavsky, W. Li and J. Xie, *ACS Applied Materials & Interfaces*, 2017, **9**, 6530-6538.
62. J. J. Richards, A. D. Scherbarth, N. J. Wagner and P. D. Butler, *ACS applied materials & interfaces*, 2016, **8**, 24089-24096.
63. S. Shukla, S. Bhattacharjee and M. Secanell, *ECS Transactions*, 2013, **58**, 1409-1428.
64. K. Malek, M. Eikerling, Q. Wang, T. Navessin and Z. Liu, *The Journal of Physical Chemistry C*, 2007, **111**, 13627-13634.
65. N. Zamel, *Journal of Power Sources*, 2016, **309**, 141-159.
66. T. T. Ngo, T. L. Yu and H.-L. Lin, *Journal of Power Sources*, 2013, **225**, 293-303.
67. J. Ning, 2016.
68. Z. Xie, T. Navessin, X. Zhao, M. Adachi, S. Holdcroft, T. Mashio, A. Ohma and K. Shinohara, *ECS Transactions*, 2008, **16**, 1811-1816.
69. J.-H. Kim, H. Y. Ha, I.-H. Oh, S.-A. Hong and H.-I. Lee, *Journal of power sources*, 2004, **135**, 29-35.
70. S. Thanasilp and M. Hunsom, *Fuel*, 2010, **89**, 3847-3852.
71. C.-Y. Jung, W.-J. Kim and S.-C. Yi, *international journal of hydrogen energy*, 2012, **37**, 18446-18454.
72. M. M. Forouzan, C.-W. Chao, D. Bustamante, B. A. Mazzeo and D. R. Wheeler, *Journal of Power Sources*, 2016, **312**, 172-183.
73. S. J. Haward, G. H. McKinley and A. Q. Shen, *Scientific reports*, 2016, **6**.
74. B. Keshavarz, E. C. Houze, J. R. Moore, M. R. Koerner and G. H. McKinley, *Physical review letters*, 2016, **117**, 154502.
75. S. H. Spiegelberg and G. H. McKinley, *Journal of Non-Newtonian Fluid Mechanics*, 1996, **67**, 49-76.
76. A. A. Potanin, R. D. Rooij, D. V. d. Ende and J. Mellema, *The Journal of Chemical Physics*, 1995, **102**, 5845-5853.
77. D. Liu, L. C. Chen, T. J. Liu, W. B. Chu and C. Tiu, *Energy Technology*, 2017.

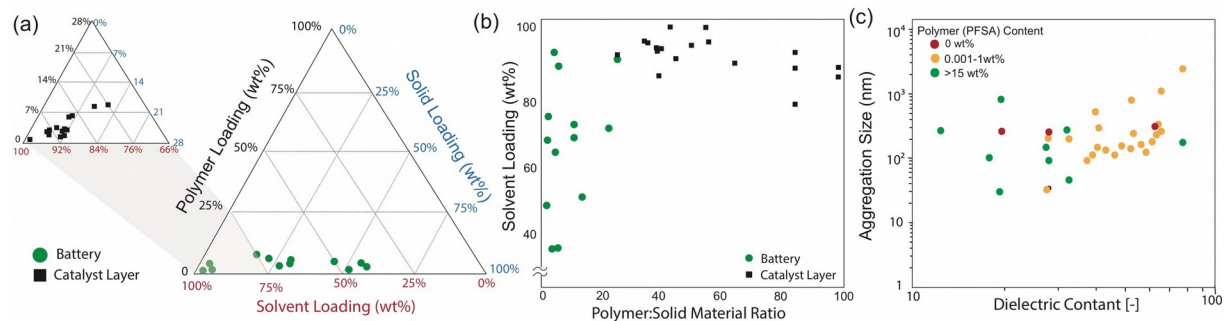


Figure 2. Ink formulations for electrodes for battery and catalyst layer applications (a) and polymer:solid content loading (b). The primary component in an ink is the solvent, and the solid aggregation size has been connected to the dielectric constant of the solvent. Data plots extracted from references 6,12,13,34,36,51,55,56,66,69-72, and 77.

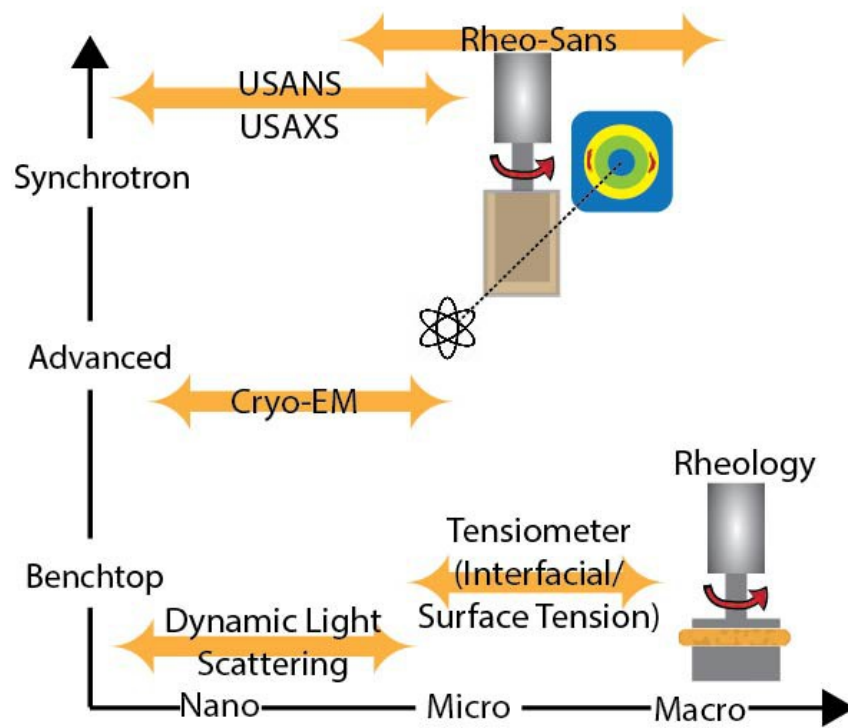


Figure 3. Multiscale processing techniques available for ink systems.

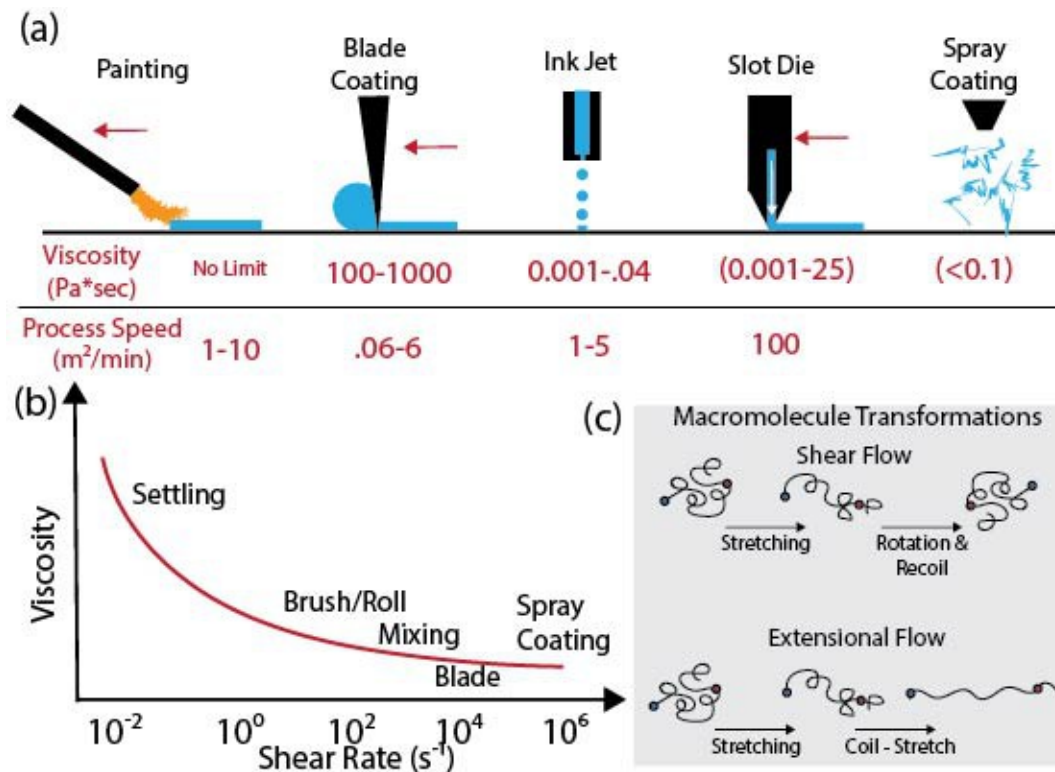


Figure 4. Examples of different processing methods relevant to electrode manufacturing (a) and the subsequent shear regimes exposed to the ink (b). High shear-rate processing characteristics of spray coating applications can lead to extension flow dynamics (c).

Table of Contents Graphic

